arXiv:1510.07960v1 [cond-mat.stat-mech] 27 Oct 2015

Phase Diagram of Twist Storing Lattice Polymers in Variable Solvent Quality

E Dagrosa[1], A L Owczarek[1] and T Prellberg[2]

[1] School of Mathematics and Statistics, The University of Melbourne, Parkville, Vic 3010, Australia.

[2] School of Mathematical Sciences, Queen Mary University of London, Mile End Road, London E1 4NS, UK.

E-mail: e.dagrosa@student.unimelb.edu.au, owczarek@unimelb.edu.au, t.prellberg@qmul.ac.uk

Abstract. When double stranded DNA is turned in experiments it undergoes a transition. We use an interacting self-avoiding walk on a three-dimensional fcc lattice to relate to these experiments and treat this problem via simulations. We provide evidence for a thermodynamic phase transition and examine related phase diagrams taking the solvent quality into account.

1. Introduction

Since the mid 1990s, experiments on single molecules of double stranded DNA have been performed [25]. In some of these experiments, the molecule is held torsionally constrained at a constant stretching force. Upon turning the molecule sufficiently, the DNA transitions from a regime of stretched states into the supercoiled regime. In this regime, the DNA is believed to coil around itself to form plectonemes and the torque exerted on the apparatus plateaus over the number of turns. Such an experiment is sketched in Figure 1. In between the stretched and supercoiled regime lies the so called buckled regime.

In 2008 [13] and thereafter [5], it was observed that, depending on the salinity of the solvent, the transition between the regimes becomes rather abrupt. This phenomena has been dubbed abrupt buckling transition.

In the literature, some of the mechanics of the experiments is modelled by treating DNA as a mathematical ribbon. According to the Calegarenu-White-Fuller theorem [28, 6, 7, 8, 14], this allows a decomposition of the number of turns added to the molecule, into writhe, total twist and a constant. More details on mathematical modeling of DNA in general can be found in [14, 3]. Details relating particular to the mechanics of the performed experiments, and which are relevant for this paper, are given in [4, 23, 24].

There are different approaches towards modeling such experiments. Free energy models are very phenomenological but can provide exact solutions. They allow the

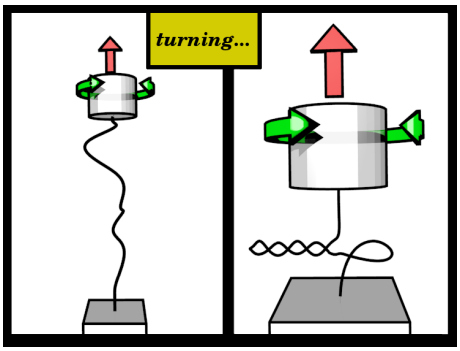

Figure 1. Sketch of an experiment that turns (green curved arrows) double stranded DNA under tension (red vertical arrow). Initially, most of the turns are expected to be absorbed in the form of twist. Due to the twist rigidity of the molecule, twisting causes the DNA to exert a restoring torque on the cylinder. Upon turning sufficiently, the DNA transitions into a regime where it is expected to form plectonemes.

inclusion of many details related to the DNA molecule. Specifically, in [12, 21, 20] the free energy is developed around three stable solutions of the elastic rod called straight, buckled and supercoiled (post-buckled). However, these models do not include potential fluctuations that are induced by correlations across the whole molecule. This makes them mathematically less interesting. Also, although in these models the buckling transition is set up to be a first-order phase transition, it is arguable that this transition is really just an abrupt transition (but not a phase transition) in a more fundamental model.

The alternative approach is to analyze the partition function directly. To obtain useful results, a basic general model must incorporate several features. Structures like plectonemes emerge only as a consequence of self-avoidance of the polymer model and also writhe (and therefore linking number) only exists for self-avoiding curves. Next, one needs to be able to pick only states of a given linking number. Finally, the ensemble needs to contain only configurations without knots. This restriction to a knot type makes it impossible to date to treat the problem analytically.

In this paper, we consider the second approach. However, we are not interested in details specific to DNA. Instead, we consider the experiment performed on the interacting self-avoiding walk (ISAW). The most famous ISAW model weights SAWs by the number of contacts between distant vertices. This model exhibits a second-order phase transition from a random coil phase into a globule phase as the quality of the solvent decreases. Variants of this model apply a pulling force which makes the collapse transition first-order [17]. Other models consider an energy cost associated with bending the walk. When the walk is sufficiently stiff, the collapse transition becomes a first order crystallization transition from the coiled phase into the crystal phase. Therefore, the phase diagram spanned by solvent quality and stiffness contains a triple point with the three phases coil, crystal and globule [2] incident.

The ISAW model used here weights unknotted SAWs on the face centered cubic

lattice by their writhe. We will argue that this relates to interpreting the SAW as a twist storing lattice polymer on which the above experiment is performed. We use the Wang-Landau-Algorithm [27] to analyze the model for scaling in the derivatives of the free energy. This allows us to infer possible phase transitions.

When the knot type is not restricted, the corresponding model has been treated by a mapping onto an $O(N \to 0)$ field theory [22]. In this work it was suggested that a sufficiently strong coupling to writhe collapses the walk. In a later work [16] a writhe induced first-order transition was predicted. In fact, we had previously performed corresponding simulations [11] and found signs of a first-order transition, which turned out to be a transition between knot types.

In this work, we find signs of a second-order transition upon weighting walks by their writhe when knot type is fixed. Although, this transition is marked by fluctuations in self-contacts, we argue that it is not the collapse transition, but a transition into a writhed phase. In addition, we consider the effect of stiffness and pulling to observe behaviour qualitatively compatible with experiments performed on DNA.

2. The Model

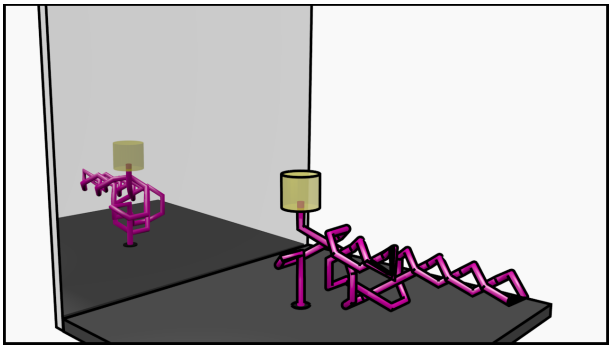

Figure 2. A sketch of a SAW on the fcc lattice. The SAW is attached to a surface and a cylinder mimicking conditions of experiments that turn TSPs.

2.0.1. Self-Avoiding Walks as Model of Twist Storing Polymers In order to model mechanics of turning a twist storing lattice polymer, we require the definition of a lattice ribbon. For our purposes, we think of a lattice ribbon $\mathcal{L} = (\varphi, V)$ as a pair formed by a self-avoiding walk (SAW) φ and a vector field V on φ, so that we have two numbers w and t that are multiples of writhe and twist, respectively. In particular, let φ be a SAW on the non-normalized face centered cubic lattice. We let φ be geometrically constrained, so that the first and last vertex lie on a given force axis and so that all vertices of φ lie in between planes through the first and last vertex. We also restrict the knot type of φ to be equivalent to the unknot.

The following provides more details. Let $O = (0, 0, 0)$ be the origin of the face-centered cubic (fcc) lattice $\Lambda = \{O + \sum_{\mathbf{k}} q_k \mathbf{k} |\, q_k \in \mathbb{Z},\, \mathbf{k} \in K\}$ where $K = \{(1, 1, 0), (1, -1, 0), ...\}$. A SAW $\varphi = \{\varphi_i\}_{i=1,..,n+1}$ of length n consists of $n+1$ connected vertices φ_i on Λ. Therefore, with $\vec{\varphi}_i := \varphi_{i+1} - \varphi_i$, $\vec{\varphi}_i^2 = 2$. Also, let $\hat{\varphi}_i := 2^{-1/2}\vec{\varphi}_i$. We anchor φ at the origin, i.e. $\varphi_1 = O$ and define a force axis $\mathbf{f} := (1, 1, 0)$. We require all vertices of the walk to lie on or above a plane that lies perpendicular to $\mathbf{f}$ through O, i.e $(\varphi_i)_x + (\varphi_i)_y \geq 0$. The last vertex, φ_{n+1} is required to lie on the axis $\varphi_{n+1} \stackrel{!}{=} O + (h-2)/2\,\mathbf{f}$, for some integer $h/2$. We then append another vertex $\varphi^{(final)} = \varphi_{n+1} + \mathbf{f}$ to the walk. This vertex has no degree of freedom so it does not count towards the length, however we require it to properly define the writhe of this non-closed walk. We imagine a second plane through $\varphi^{(f)}$ such that no vertex can lie on or above this plane, i.e. $(\varphi_i)_x + (\varphi_i)_y < 2\left(\varphi^{(final)}\right)_x$. Finally, we imagine to connect $\varphi_1 - \mathbf{f}$ and φ_{n+1} through a planar walk ν whose arch is wide enough so that its rotation ellipsoid around $\mathbf{f}$ is disjoint with φ. Then, we require that the closed polygon $\bar{\varphi} := \varphi \cup \nu$ is an unknot. Formally, the writhe of φ can be defined by the writhe of $\bar{\varphi}$, i.e. $Wr(\varphi) := Wr(\bar{\varphi})$. To compute the writhe, we use the formula

$$\begin{aligned} Wr(\varphi) \;= Lk(\bar{\varphi},\, \bar{\varphi} + \epsilon\mathbf{d}) - \frac{1}{2\pi}\sum_{i=1}^{n}\Bigg\{ & \\ \arctan\left(\frac{\langle \mathbf{d},\, \hat{\varphi}_{i-1}\rangle - \langle \mathbf{d},\, \hat{\varphi}_i\rangle\, \langle \hat{\varphi}_{i-1},\, \hat{\varphi}_i\rangle}{[\hat{\varphi}_{i-1},\, \hat{\varphi}_i,\, \mathbf{d}]}\right) & \\ + \arctan\left(\frac{\langle \mathbf{d},\, \hat{\varphi}_i\rangle - \langle \mathbf{d},\, \hat{\varphi}_{i-1}\rangle\, \langle \hat{\varphi}_{i-1},\, \hat{\varphi}_i\rangle}{[\hat{\varphi}_{i-1},\, \hat{\varphi}_i,\, \mathbf{d}]}\right)\Bigg\}, & \end{aligned} \tag{1}$$

where $Lk(\bar{\varphi},\, \bar{\varphi} + \epsilon\mathbf{d})$ is the linking number between the closed polygon $\bar{\varphi}$ and a copy of $\bar{\varphi}$ pushed off a small amount into direction $\mathbf{d}$. We set $\hat{\varphi}_0 := \hat{\mathbf{f}}$. $\langle \bullet, \bullet\rangle$ denotes the scalar product, and $[\bullet,\, \bullet,\, \bullet]$ the triple product. Using an appropriate algorithm to compute $Lk(\bar{\varphi},\, \bar{\varphi} + \epsilon\mathbf{d})$ and a proper choice for $\mathbf{d}$, one may show that writhe can be computed without taking the closure ν of $\bar{\varphi}$ into account. We have derived the formula 1 in [10]. Alternative expressions for the writhe of polygonal curves can be found in [18, 15, 1], however some of these are not appropriate for the kind of simulation performed here. For reasons explained in the next section, we use the observables $w = 30\,Wr(\varphi)$, $t = 30\,Tw(V, \varphi)$ and $l = w + t$.

Furthermore, let $h = 2\left(\varphi^{(final)}\right)_x$ measure $\sqrt{2}$ times the distance of the final vertex from O. Let c denote the number of contacts between vertices and let $s = n + \sum_i \langle \vec{\varphi}_i,\, \vec{\varphi}_{i+1}\rangle$ denote the number of stiff sites. Note that $s \in [0,\, 3n]$. We hold the temperature T fixed and define the energy of a configuration $\mathcal{L}$ by

$$E(\mathcal{L}) = const - k_B T\,(\beta_h h + \beta_c c + \beta_s\, s + \beta_t\, t),$$

where the coupling β_h is related to pulling force, β_s to stiffness (bending energy), β_t to twist rigidity and β_c can be related to the quality of the solvent. We remark that the subscripts to the betas are merely a pairing label, not an index, i.e., β_c does not depend

on c. To keep notation short, we collect some of the observables as $\mathbf{m} = (s,\, h\, c)^T$ and the corresponding couplings as $\vec{\beta} = (\beta_s,\, \beta_h,\, \beta_c)^T$. We denote the density of states by $C^{(Rib)}_{n\,\mathbf{m}\,w\,t}$, so that the partition function of the constant linking number l ensemble is given by

$$Z^{(Rib)}_{n\,l}\left(\beta_t,\, \vec{\beta}\right) = const \sum_w \sum_t \sum_{\mathbf{m}} C^{(Rib)}_{n\,\mathbf{m}\,w\,t}\, e^{\vec{\beta}\cdot\mathbf{m}} e^{\beta_t t} \delta_{l,\,w+t},$$

where, using the CFW theorem, $\delta_{l,\,w+t}$ picks only the ribbons that have linking number l. Discrete Laplace transformation of $Z_{n\,l}$ with respect to l yields the conjugated fully canonical ensemble of ribbons

$$\begin{aligned} Z^{(Rib)}_{n}\left(\beta_t,\, \vec{\beta},\, \beta_l\right) &= \sum_l Z^{(Rib)}_{n\,l}\left(\beta_t,\, \vec{\beta}\right) e^{\beta_l l} \\ &= const \sum_w \sum_t \sum_{\mathbf{m}} C^{(Rib)}_{n\,\mathbf{m}\,w\,t}\, e^{\vec{\beta}\cdot\mathbf{m}} e^{\beta_l w} e^{(\beta_t+\beta_l)t}, \end{aligned}$$

where β_l is related to torque. This ensemble corresponds to an experiment that keeps the polymers under a fixed torque rather than linking number. Therefore, we refer to it as the constant torque ensemble. So far, we have not specified how the vector field V should look. Suppose that a rule of constructing V is such that the number of ribbon frames with total twist t, i.e. C_t is independent of φ, then

$$C^{(Rib)}_{n\,\mathbf{m}\,w\,t} = C_{n\,\mathbf{m}\,w} C_t, \tag{2}$$

and the partition function factors according to

$$Z^{(Rib)}_{n}\left(\beta_t,\, \vec{\beta},\, \beta_l\right) = Z^{(Wr)}_{n}\left(\vec{\beta},\, \beta_l\right) Z^{(Tw)}_{n}\left(\beta_t,\, \beta_l\right), \tag{3}$$

where

$$Z^{(Wr)}_{n}\left(\vec{\beta},\, \beta_l\right) = \sum_w \sum_{\mathbf{m}} C_{n\,\mathbf{m}\,w}\, e^{\vec{\beta}\cdot\mathbf{m}} e^{\beta_l w} \tag{4}$$

and $Z^{(Tw)}_{n}\left(\beta_t,\, \beta_l\right) = const \sum_t C_t e^{(\beta_t+\beta_l)t}$. As we are interested in the singularity structure of the free energy $f^{(Rib)} = \lim_{n\to\infty} f^{(Rib)}_n$, the factoring (3) of the partition function implies that we may examine the scaling of the derivatives of $f^{(Wr)}_n\left(\beta_t,\, \vec{\beta},\, \beta_l\right) = n^{-1} \log Z^{(Wr)}_n$ and $f^{(Tw)}_n$ independently to obtain information of the potential critical points of the system. However, because total twist is a quantity that is computed along the walk, we do not expect any singularities associated with $f^{(Tw)}$. Consequently, we can focus on (4), which only requires us to perform simulations of a SAW rather than a ribbon. We note that even in the case $\vec{\beta} = 0$, our partition function $Z^{(Wr)}_n$ contains a Boltzmann factor $\exp\left(\beta_l\, w\right)$, where the writhe w is obtained by relating near and distant parts of the walk to each other. Therefore, the torque β_l can induce long distance correlations across the polymer. But this means that the system might potentially become critical. In fact, we have examined the partition function $\sum C_{n\,w} e^{\beta_l w}$ in systems which do not preserve the topology [11]. In this case, we found a first-order transition between knot types associated with the partition function.

We recall that the convenient factorization (3) is due to two reasons. First, we work in the conjugated constant torque ensemble. In the thermodynamic limit $n \to \infty$, the ensembles are equivalent so that any inference we make about phase transitions should also hold in the linking number ensemble. The second reason is relation (2). Although, we can certainly make a rule so that (2) holds, it is not necessarily natural on the fcc lattice. However, the resulting factoring of the partition function (3) is also obtained in continuous models of dsDNA. For example, compare (3) to formula (6) in [23], where the ribbon frame is attached to the continuous worm like chain model. Therefore, imposing condition (2) yields a simple model compatible with non-lattice models in the literature.

2.1. Algorithm and Data

2.1.1. Algorithm Let t be the algorithm time, then, at given length n, the Wang-Landau Algorithm (WLA) can be used to obtain an estimate $s^{(est)}_{n\,w\,\mathbf{m}}(t)$ of the microcanonical entropy

$$s_{n\,w\,\mathbf{m}} := \log C_{n\,w\,\mathbf{m}}\,,$$

where one expects that for large enough times $s^{(est)}_{n\,w\,\mathbf{m}}(t) \approx const\, t + s_{n\,w\,\mathbf{m}}$. We can consider the WLA as a pair $\left(\varphi(t),\, s^{(est)}_{n\,w\,\mathbf{m}}(t)\right)$, where $\varphi(t)$ is the current state of the algorithm. A step of the WLA algorithm consists in proposing a state φ^* to the WLA, which is accepted with the probability

$$p_{acc} = \min\left[1,\, \exp\left\{s^{est}_{w(t)\,\mathbf{m}(t)}(t) - s^{est}_{w^*\mathbf{m}^*}(t)\right\}\right], \tag{5}$$

where $s^{est}_{w(t)\,\mathbf{m}(t)}(t)$ is the value of $s^{(est)}_{n\,w\,\mathbf{m}}(t)$ at $w = w(t)$ and $\mathbf{m} = \mathbf{m}(t)$. Therefore,

$$\varphi(t+1) = \begin{cases} \varphi^* & p \le p_{acc}, \\ \varphi(t) & else. \end{cases}$$

Finally, $s^{(est)}_{n\,w\,\mathbf{m}}(t)$ is updated as $s^{(est)}_{n\,w\,\mathbf{m}}(t+1) = s^{(est)}_{n\,w\,\mathbf{m}}(t) + \log f\, \delta_{w\,w(t+1)}\delta_{\mathbf{m}\,\mathbf{m}(t+1)}$, where f is called the modification factor. For large t the modification factor is reduced as $\log f \sim 1/t$. Instead of using the traditional method we will use a modification of the WLA to obtain estimates for

$$s_{n\,w}\left(\vec{\beta}\right) := \log\left\{\sum_{\mathbf{m}} C_{n\,w\,\mathbf{m}} e^{\vec{\beta}\cdot\mathbf{m}}\right\}. \tag{6}$$

These are obtained by changing the acceptance probability to

$$p_{acc} = \min\left[1,\, \exp\left\{s^{est}_{w(t)}(t) - s^{est}_{w^*}(t) + \vec{\beta}\cdot(\mathbf{m}^* - \mathbf{m}(t))\right\}\right]. \tag{7}$$

One obtains φ^* from $\varphi(t)$ by applying a move on $\varphi(t)$. We use three kinds of move:

Bond Flip A vertex φ_i is selected randomly. It is randomly moved onto one of the lattice sites that neighbor both φ_{i-1} and φ_{i+1}.

Kink Transport A vertex φ_i is selected randomly. If φ_{i-1} and φ_{i+1} are neighbors φ_i is removed and inserted either between two different vertices or it is appended at the end in $\hat{\mathbf{f}}$ direction.

End to Kink When the last step of the walk lies in $\hat{\mathbf{f}}$ direction, the last vertex can be removed and inserted between two vertices of the SAW.

We note that every move has its inverse move. The moves are applied randomly, but in a way that detailed balance is satisfied. When a move yields a state that is not in the ensemble, for example the state is not self-avoiding, we set $\varphi^* = \varphi(t)$. The authors in [26] assumed that the combination of bond-flips and kink-transport (pull moves for a SAP) are ergodic within the knot type of a polygon on the sc lattice. We will assume the same to be true for the restricted walk on the fcc lattice considered here. One can easily convince oneself that the move set is ergodic within the desired ensemble for length $n \leq 4$. In dealing with the WLA, it is common practice to split the space of macrostates $\Gamma = \{w_1, w_2, ..., w_{max}\}$ into overlapping subsets Γ_i where $\Gamma = \bigcup_i \Gamma_i$ and $\Gamma_i \cap \Gamma_{i+1} \neq \emptyset$ and generate estimates $s^{(i)}_{n\,w}\left(\vec{\beta},\, t^{(i)}\right)$ over Γ_i. This requires restricting $\varphi^{(i)}\left(t^{(i)}\right)$ so that $w^{(i)}\left(t^{(i)}\right) \in \Gamma_i$. However, particularly for some $\vec{\beta}$ far away from 0, this method works very poorly and it becomes essential to parallelize the WLAs $WLA^{(i)}\left(t^{(i)}\right) = \left(\varphi^{(i)}\left(t^{(i)}\right),\, s^{(i)}_{n\,w}\left(\vec{\beta},\, t^{(i)}\right)\right)$ by introducing an additional move. Consider two pairs of Wang-Landau algorithms $WLA^{(i)}\left(t^{(i)}\right)$ and $WLA^{(j)}\left(t^{(j)}\right)$. Denote by t a global time, so that at this time the corresponding chains are in the states $\varphi^{(i)}\left(t^{(i)}(t)\right)$ and $\varphi^{(j)}\left(t^{(j)}(t)\right)$ respectively. For now, denote by $w^{(i)}(t)$ the writhe of $\varphi^{(i)}\left(t^{(i)}(t)\right)$ and by $s^{(i)}_{w^{(j)}}$ the current estimate of $s^{(i)}_{w}$ at $w = w^{(j)}(t)$. Then, when the algorithms $WLA^{(i)}$ and $WLA^{(j)}$ overlap at global time t, i.e. $w^{(i)}(t),\, w^{(j)}(t) \in \Gamma^{(i)} \cap \Gamma^{(j)}$ a chain switch is performed with probability

$$p_{acc} = \min\left[1,\, \exp\left\{s^{(i)}_{w^{(i)}} - s^{(i)}_{w^{(j)}} + s^{(j)}_{w^{(j)}} - s^{(j)}_{w^{(i)}}\right\}\right], \tag{8}$$

so that

$$\varphi^{(i)}\left(t^{(i)}+1\right) = \begin{cases} \varphi^{(j)}\left(t^{(j)}\right) & p \leq p_{acc}, \\ \varphi^{(i)}\left(t^{(i)}\right) & else. \end{cases} \tag{9}$$

The details of this procedure were suggested in [19], where it was shown to be very helpful on some benchmark problems. In our case, it is essential to overcome the trapping of the walk $\omega^{(i)}$ in regions of the state space that are not representative enough to produce a good estimate of the entropy.

2.1.2. Data We ran several simulations to obtain estimates for $s_{n\,w}(\beta_s,\, \beta_h,\, \beta_c)$ and $s_{n\,c}(\beta_l,\, \beta_s,\, \beta_h)$. Although writhe assumes discrete values on the fcc lattice, the macrostates labeled by w lie very dense, thus the estimates of $s_{n\,w}$ are made using $w \leftarrow round(abs(w))$ and taking advantage of the symmetry $s_{n\,w} = s_{n\,-w}$. Recall that $w := 30\,Wr$, so that 30 serves as the resolution for the estimates of $s_{n\,w}$. This resolution factor was determined, as $round(abs(30\,Wr))$ allows to just resolve the state

of maximum writhe of self-avoiding polygons on the fcc lattice. As an example of the results, Figure 3 shows the estimated entropies $s_{n=192\,w}\,(\beta_s=0,\,\beta_h=0,\,\beta_c=0)$ and $s_{n=192\,c}\,(\beta_l=0,\,\beta_s=0,\,\beta_h=0)$.

As we are interested in the potentially critical points in coupling space $(\beta_l,\,\beta_s,\,\beta_h,\,\beta_c)$ we want to observe the scaling of the derivatives of the free energy $f_n^{(Wr)}$. With $m=l,\,c,\,s,\,...$ define

$$f_n^{m_1,\,m_2...,\,m_k}\left(\beta_l,\,\vec{\beta}\right):=\left(\frac{\partial^k}{\partial\beta_{m_1}\partial\beta_{m_2}...\partial\beta_{m_k}}f_n^{(Wr)}\left(\beta_l,\,\vec{\beta}\right)\right)^{(est)}, \tag{10}$$

where for example $f_n^l=n^{-1}\left\langle w\right\rangle_n^{(est)}\left(\beta_l,\,\vec{\beta}\right)$, which can be computed as

$$\left\langle w\right\rangle_n^{(est)}\left(\beta_l,\,\vec{\beta}\right)=\frac{\sum_w w\,e^{\beta_l\,w+s_{n\,w}^{(est)}\left(\vec{\beta}\right)}}{\sum_w e^{\beta_l\,w+s_{n\,w}^{(est)}\left(\vec{\beta}\right)}}. \tag{11}$$

In the same way one uses $s_{n\,w}^{(est)}\left(\vec{\beta}\right)$ to compute all derivatives with respect to β_l, i.e. $f_n^l,\,f_n^{l\,l},\,\ldots$. To obtain the estimates $f_n^m,\,f_n^{m\,m}$ with $m\neq l$, note that for a generic function $g\,(w,\,\mathbf{m})$

$$\begin{aligned}\left\langle g\,(w,\,\mathbf{m})\right\rangle_n\left(\beta_l,\,\vec{\beta}\right)&:=\frac{\sum_w e^{\beta_l w}\sum_{\mathbf{m}}g\,(w,\,\mathbf{m})\,e^{\vec{\beta}\cdot\mathbf{m}+s_{n\,w\,\mathbf{m}}}}{\sum_w e^{\beta_l w}\sum_{\mathbf{m}}e^{\vec{\beta}\cdot\mathbf{m}+s_{n\,w\,\mathbf{m}}}}\\&=\frac{\sum_w e^{\beta_l w}\left\langle g\,(w,\,\mathbf{m})\right\rangle_w e^{s_{n\,w}\left(\vec{\beta}\right)}}{\sum_w e^{\beta_l w+s_{n\,w}\left(\vec{\beta}\right)}},\end{aligned} \tag{12}$$

where $\left\langle g\,(w,\,\mathbf{m})\right\rangle_w=\sum_{\mathbf{m}}g\,(w,\,\mathbf{m})\,e^{\vec{\beta}\cdot\mathbf{m}+s_{n\,w\,\mathbf{m}}-s_{n\,w}\left(\vec{\beta}\right)}$. We obtain estimates for $\left\langle m\right\rangle_w$ as the sample averages $\left\langle m\right\rangle_w^{(est)}:=N_{Samples}^{-1}\sum_{i=1}^{N_{Samples}}m\,(w\,(t_i)=w)$. Therefore, every time $\varphi\,(t)$ has writhe w, we take a sample $m\,(\varphi\,(t_i))$. In the same way we obtain estimates of $\left\langle m^2\right\rangle_w^{(est)}$. In addition to the parameters $m=c,\,s,\,w$, we will also keep track of the moment of inertia with respect to the force axis. It is given as

$$I\,(\varphi)=\frac{1}{n}\sum_i\left\{\varphi_i^2-\frac{1}{2}\left(\left[\varphi_i\right]_x^2+\left[\varphi_i\right]_y^2\right)\right\}. \tag{13}$$

When the states φ^* proposed to the algorithm are drawn according to the probability distribution the form of the error is well known and statistical [29]. However, in our case, the states φ^* are proposed by applying a move to $\varphi\,(t)$. This is usually associated with an unknown systematic error related to the move set. Yet, one hopes that that the error decays with the modification factor $\log f\sim 1/t$. We also expect some residual boundary effect error due to the splitting of Γ into Γ_i. Finally, we expect a statistical error associated with combining the $s_{n\,w}^{(i)}\left(t^{(i)}\right)$ to form $s_{n\,w}^{(est)}$. In conclusion, we can not predict the form of the error, so we form a naive standard error. Therefore we provide standard confidence intervals for $f_n^{l\,l}\left(\beta_l,\,\vec{\beta}\right)$ by averaging over several $s_{n\,w}^{(est)}$. These estimates are obtained at different global times, but with small enough modification factor. Typically, it is required that $\log\,(f)<10^{-8}$.

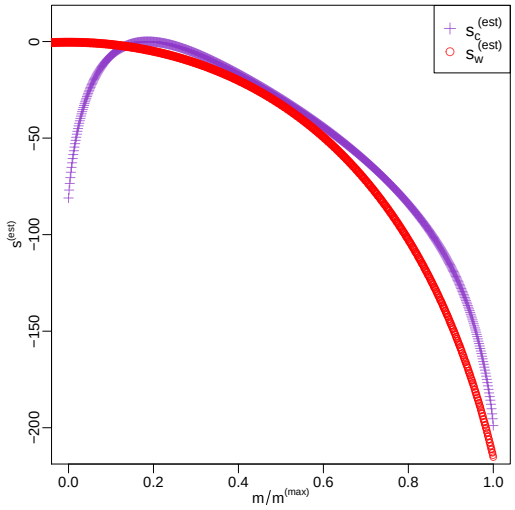

Figure 3. Shown are entropies over $c/715$ and over $w/1020$ at $n = 192$. We note that $w^{(max)} = 1020$ is the value of the cut off and not the actual maximal value of the writhe w. Using the asymptotic formula [9] $\lim_{n\to\infty} Wr^{max}/n = \frac{1}{2\pi} \arctan\left(2\sqrt{2}\right)$ for the maximum writhe of an unknot on the fcc lattice, we expect the maximum w near 1128.

3. Results

3.1. Flexible polymers without pulling

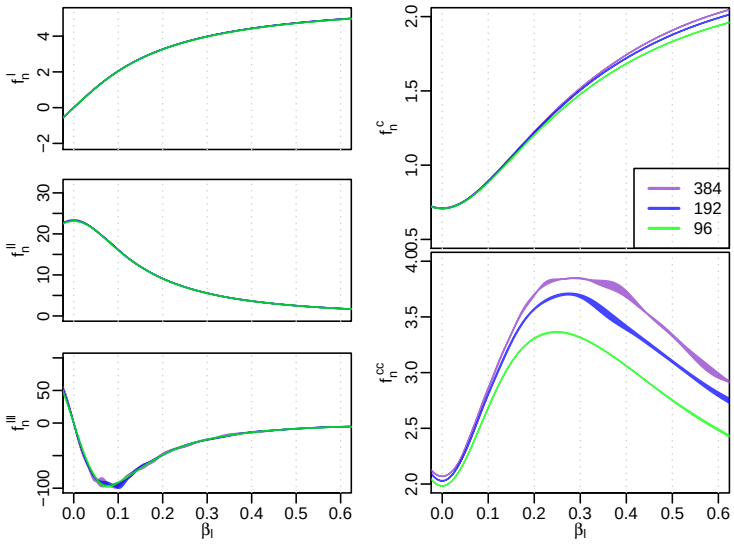

Figure 4. Scaling of the first three derivatives of the free energy with respect to β_l against β_l and the first two derivatives with respect to β_c. The curves of f_n^l, f_n^{ll} and f_n^{lll} are almost identical at the considered lengths 384, 192 and 96.

First we consider the case of flexible lattice polymer that are not being pulled

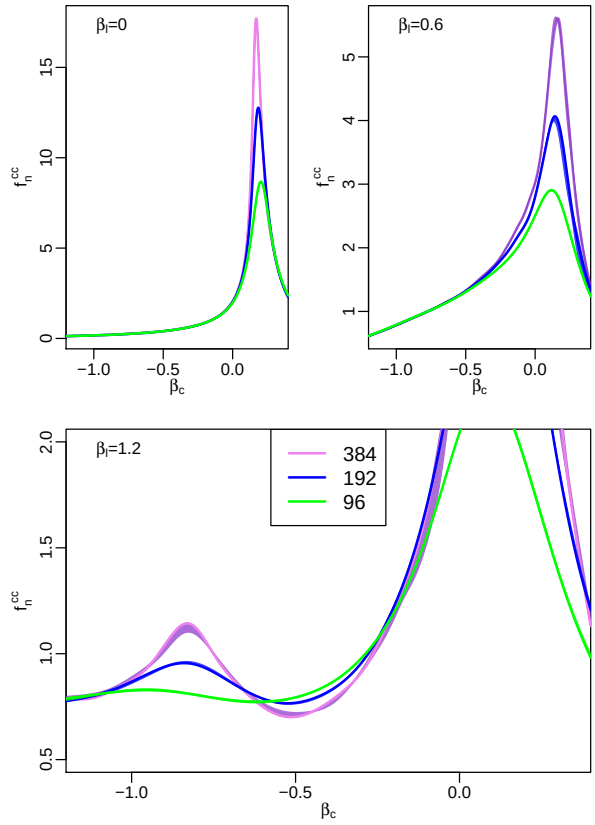

Figure 5. Scaling of $f_n^{cc}(\beta_l = const, \beta_c, \beta_s = 0, \beta_h = 0)$ at different torques $\beta_l = \{0, 0.6, 1.2\}$.

$(\beta_s = 0, \beta_h = 0)$. The left-hand side graphs in Figure 4 show the scaling of the first, second and third derivatives of the free energy with respect to β_l against the torque β_l. None of the derivatives shows any signs of non-trivial scaling. The graphs on the right-hand side in Figure 4 show the estimates for the first and second derivative with respect to β_c. The graphs of $f_n^{cc}(\beta_l)$ have a peak between $\beta_l = 0.2$ and $\beta_l = 0.4$. The height of the peak $f_n^{cc}(\beta_l)$ increases with n. However, the scaling is somewhat unusual because the scaling region extends far to the right of the peak position. Nevertheless, we conjecture that this scaling is associated with a continuous phase transition, for which we associate the position of the peak with the location of the transition. In the following we will provide additional evidence for this transition by considering the problem in the β_c-β_l plane.

Figure 5 shows the scaling $f_n^{cc}(\beta_c, \beta_l = const)$ at different torques. At $\beta_l = 0$ one observes scaling around $\beta_c = 0.2$, which is compatible with a second-order phase transition. The transition can be identified with the familiar collapse transition from the coil into the globule phase. As the torque is increased a transition into the globule phase persists around $\beta_c = 0.2$. In addition to this transition, Figure 5 shows that at $\beta_l = 1.2$, scaling around $\beta_c = -0.8$ emerges. This scaling is potentially compatible with an additional continuous phase transition. At the considered lengths, we do not

find signs of this latter transition in $f_n^{cc}(\beta_c,\, \beta_l = const)$ when $\beta_l \leq 0.8$. However, we conjecture that this transition is related to the peak in $f_n^{cc}(\beta_l,\, \beta_c = 0)$ to form the finite size phase diagram sketched in Figure 6.

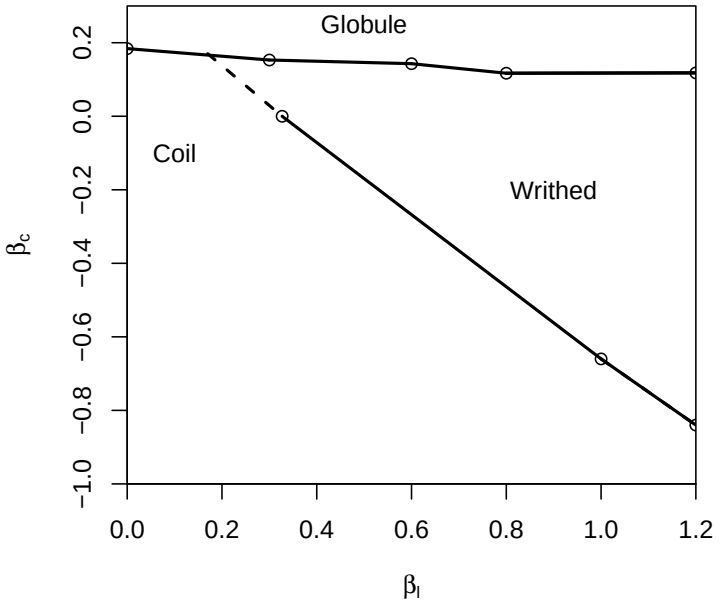

Figure 6. Finite size schematic phase diagram at $\beta_s = 0$, $\beta_h = 0$. The circles correspond to the positions of peaks in $f_{n=192}^{cc}$. The solid lines are linear interpolation between the circles and represent the phase boundaries. The dotted line is a linear interpolation of the coil-writhed phase boundary. It meets the coil-globule transition at the conjectured triple point near ($\beta_l = 0.17$, $\beta_c = 0.17$). No line in this diagram is expected to correspond to a first-order transition.

We estimate a triple point near ($\beta_l = 0.17$, $\beta_c = 0.17$) where the three phases coil, globule and writhed are incident. The writhed phase is the conjectured phase, which encompasses the states of intermediate and high writhe but which are not part of the globule phase. One notes that all transitions: coil-globule, coil-writhed and writhed-globule are associated with contact fluctuations. When the transitions are close in the space of couplings, we can imagine that the associated fluctuations overlap. Therefore it is not possible to locate the coil-writhed transition, as it is overpowered by the fluctuations associated with the writhed-globule transition. It is known that the contact fluctuations diverge logarithmically across the collapse transition. If this is also true for the writhed-globule transition, and assuming that the fluctuations associated with the coil-writhed transition do not diverge, then in general we can not expect to resolve the coil-writhed transition in $f_n^{cc}(\beta_c,\, \beta_l = const)$ at any length when the writhed-globule transition lies close.

Consider the effect of negative β_c. First, negative β_c corresponds to a repulsion between neighboring monomers and thus a swelling of the chain. However, the repulsion is short range, that is one lattice unit. Therefore, as the length is increased, this effect becomes negligible compared to the swelling due to the entropy.

The second effect of negative β_c is the suppression of $2\,\pi/3$ angles between bonds. These correspond to kinks, i.e. local configurations where two next nearest vertices of the SAW are one lattice step apart. Thus, negative β_c forces a certain type of stiffness on the lattice polymer. As discussed above, stiffness has a non-trivial effect on the collapse transition. We also expect stiffness to be relevant to writhe. Therefore, we will consider stiff (semi-flexible) polymers in the following.

3.2. Semi-flexible pulled polymers

We now consider the case of semi-flexible polymers ($\beta_s > 0$) being subject to a strong pulling force. This makes it is easier to converge the estimates $s_{n\,w}^{(est)}\left(\vec{\beta}\right)$ (and in particular $s_{n\,c}^{(est)}\left(\vec{\beta}\right)$) properly. Also, the case of semi-flexible, pulled polymers corresponds to the situation in experiments on dsDNA.

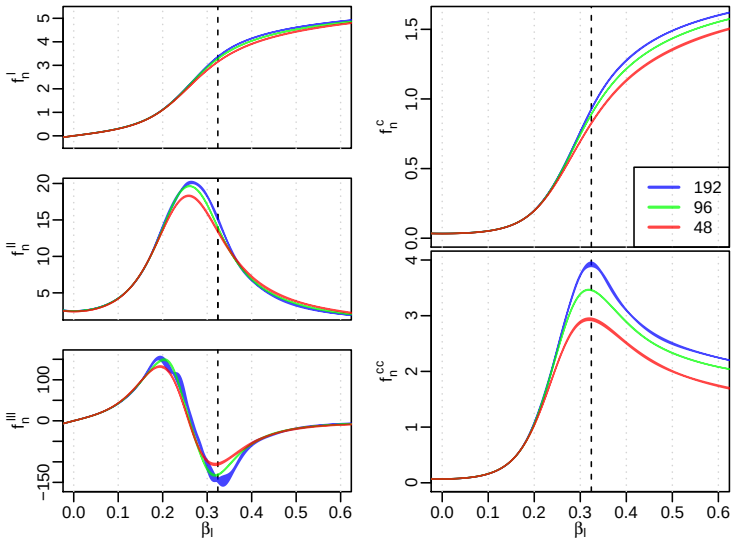

Figure 7. The graphs on the left-hand side depict the scaling of the estimates for first three derivatives of the free energy with respect to β_l and against β_l. The two graphs on the right-hand side show the corresponding scaling of the first two derivatives with respect to β_c. The couplings are held fixed at ($\beta_c = 0$, $\beta_s = 1$, $\beta_h = 0.5$). The vertical line on the left graphs marks the position ($\beta_l^* = 0.247$) of the peak in $f_{n=192}^{cc}$. We interpret the scaling of the observables as a second-order stretched-writhed transition.

Figure 7 shows the derivatives at $\beta_s = 1$ and $\beta_h = 0.5$ against torque. In contrast to the previous case (figure 4), we now detect scaling in f_n^{ll} and f_n^{lll}, such that the negative peak in the third derivative might diverge in the thermodynamic limit (at least when

the polymer is stiff enough). Other than the scaling in f_n^{cc}, the scaling in f_n^{ll} and f_n^{lll} is localized and restricted to the peak area. We find that the position of the negative peak in f_n^{lll} coincides with the peak in f_n^{cc}. This establishes further justification for having identified the peak in f_n^{cc} in Figure 4 with the position of the transition to produce the above phase diagram (6). In order to produce the phase diagram for the stiff and pulled polymer, we obtain the positions of the transitions either from the negative peak in $f_n^{lll}(\beta_l, \beta_c = const)$ or the peaks in $f_n^{cc}(\beta_l = const, \beta_c)$. The resulting phase diagram is shown in Figure 8.

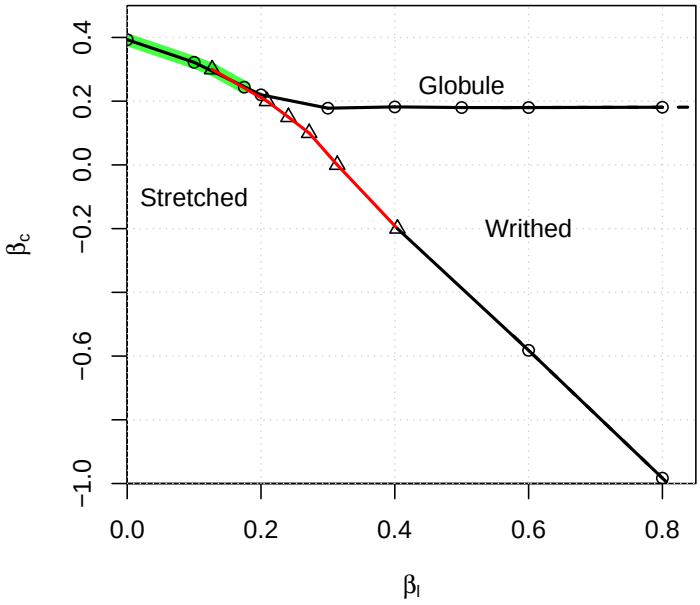

Figure 8. Finite size ($n = 96$) phase diagram at $\beta_s = 1$, $\beta_h = 0.5$. The black lines represent the phase boundaries when determined from peaks in f_n^{cc}, the red line when determined from the negative peaks in f_n^{lll}. The thick (green) line represents a line of confirmed first-order transitions. The transition is second-order at $\beta_l = 0.2$.

Due to the pulling, the coil-globule transition has become a first order stretched-globule transition. The stretched phase is usually characterized by a scaling exponent defined by $\langle h \rangle_n \sim n^{\zeta_h}$ where $\zeta_h = 1$ as opposed to $\zeta_h = \nu_{SAW} \approx 0.59$ when no pulling force is applied. This is shown in Figure 9 which shows an estimate for

$$\zeta_h^{(n)}(\beta_l) := \frac{\log\left(\langle h \rangle_{2n} / \langle h \rangle_n\right)}{\log(2)} \tag{14}$$

at $n = 48$ and $\beta_h = 0$, 0.5. Clearly, the result is compatible with $\zeta_h = 1$ at $\beta_h = 0.5$.

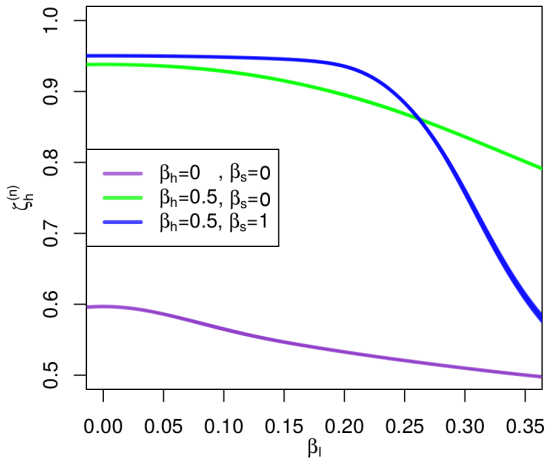

Figure 9. Estimate for $\zeta_h^{(n)}(\beta_l)$ at $n = 48$ and different values of the pulling force: $\beta_h = 0$ and $\beta_s = 0$ (bottom), $\beta_h = 0.5$ and $\beta_s = 0$ (middle), and $\beta_h = 0.5$ and $\beta_s = 1$ (top). Changing to non-zero β_h increases the exponent from values around 0.59 to a value close to 1 for small β_l, consistent with a stretched phase.

The phase diagram in Figure 8 is associated with three transitions. The stretched-globule, stretched-writhed and writhed-globule transition. We will examine these transitions in the following.

In Figures 7, 10, and 11, we show transitions out of the stretched phase by applying torque at different values of β_c. We have already discussed the case $\beta_c = 0$ in Figure 7, where we pass through the stretched-writhed transition. At $\beta_c = 0.3$, we pass through the stretched-globule transition. The derivatives of the free energy are shown in Figure 11. We point out that not only does the number of contacts behave like a discontinuous order parameter, but also writhe fluctuations per length appear to scale linearly with the length. This of course confirms that the stretched-globule transition remains first-order when some torque is applied. Figure 10 considers the transition near the triple point. By setting $\beta_c = 0.15$ we begin in the stretched phase at low torque and end up in the writhed phase at high torque. The scaling is compatible with a second-order phase transition. It is clearly more pronounced than at $\beta_c = 0$.

Figure 12 shows the behavior of the number of stiff sites and the extension across the transitions. Both observables decrease across the transitions. The decrease is more abrupt across the stretched-globule transition and takes an intermediate value for $\beta_c = 0.15$.

We will now examine the writhed-globule transition at fixed torque $\beta_l = 0.4$. However, we will consider the case of even less flexible polymers ($\beta_s = 2$) as this will help to resolve the stretched-writhed from the writhed-globule transition near the triple point. Figure 13 shows derivatives of the free energy over β_c at $\beta_l = 0.4$, $\beta_s = 2$, $\beta_h = 0.5$. One observes two peaks in the fluctuations of the number of contacts f_n^{cc}.

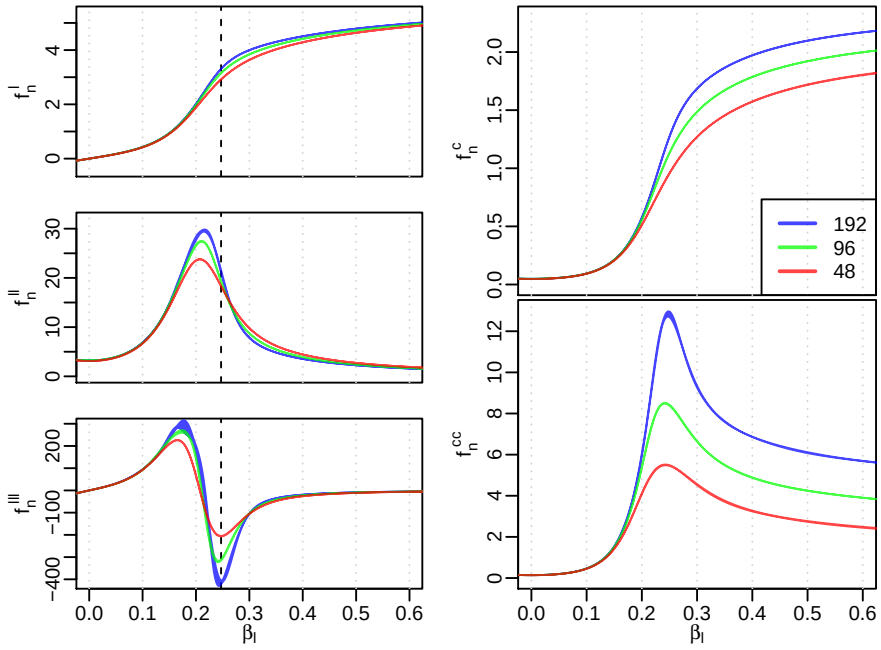

Figure 10. The graphs on the left-hand side depict the scaling of the estimates for first three derivatives of the free energy with respect to β_l and against β_l. The two graphs on the right-hand show the corresponding scaling of the first two derivatives with respect to β_c. The couplings are held fixed at ($\beta_c = 0.15$, $\beta_s = 1$, $\beta_h = 0.5$). The vertical line on the left graphs marks the position ($\beta_l^* = 0.247$) of the peak in $f^{cc}_{n=192}$. We interpret the scaling of the observables as a second-order stretched-writhed transition.

We associate the first peak with the stretched-writhed transition and the second peak with the writhed-globule transition. We have marked the positions of the transitions by vertical lines. The bottom right graph shows that only the stretched-writhed transition is associated with writhe fluctuations. Compared to the case at $\beta_s = 1$ (in Figure 7) the writhe fluctuations grow more strongly with length. Therefore, one may wonder whether this transition becomes first-order for even stiffer polymers. It is interesting to note from the top right graph that the writhe actually grows across the writhed phase so that it takes its highest value in the globule phase. We expect the state of maximum writhe to be a plectoneme in the writhed phase, so that at very high β_l, we would expect a small dip in the writhe when transitioning into the globule phase.

Figure 14 shows the moment of inertia against β_c. In contrast to all other considered observables, the moment of inertia truly behaves distinctly (only for stiff, pulled polymers) in the writhed phase as it takes its maximum value here and falls off towards the stretched and globule phase, respectively. This is consistent with the formation of (loose) plectonemic structures which extend away from the axis, as for example shown in Figure 2.

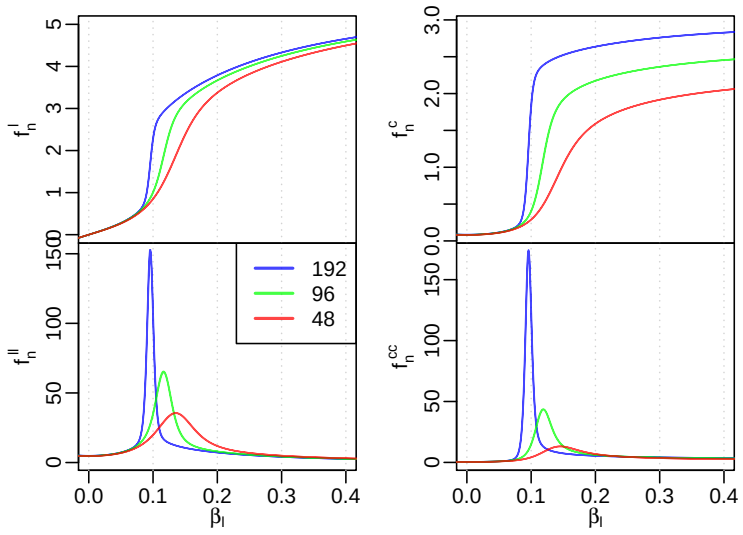

Figure 11. The graphs on the left-hand side depict the scaling of the estimates for first two derivatives of the free energy with respect to β_l and against β_l. The two graphs on the right-hand show the corresponding scaling of the first two derivatives with respect to β_c. The couplings are held fixed at ($\beta_c = 0.30$, $\beta_s = 1$, $\beta_h = 0.5$). We interpret the scaling of the observables as the first-order collapse transition (stretched-globule transition).

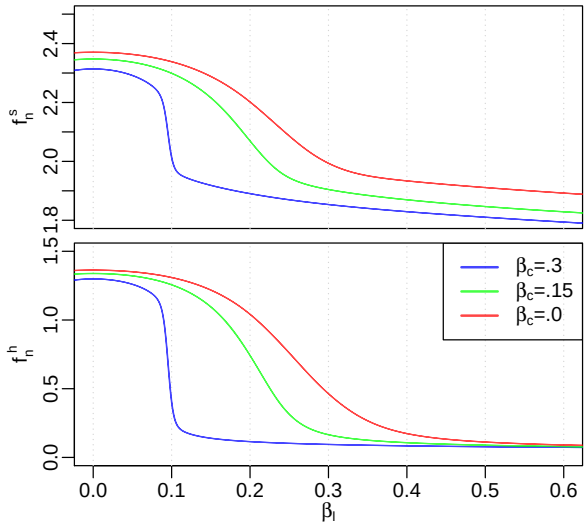

Figure 12. Expectation values per length of the number of stiff sites f_n^s and extension f_n^h at $n = 192$ and values $\beta_c = 0, 0.15, 0.3$, where the upper curves in each graph corresponds to $\beta_c = 0$ and the lowest curves corresponds to $\beta_c = 0.3$.

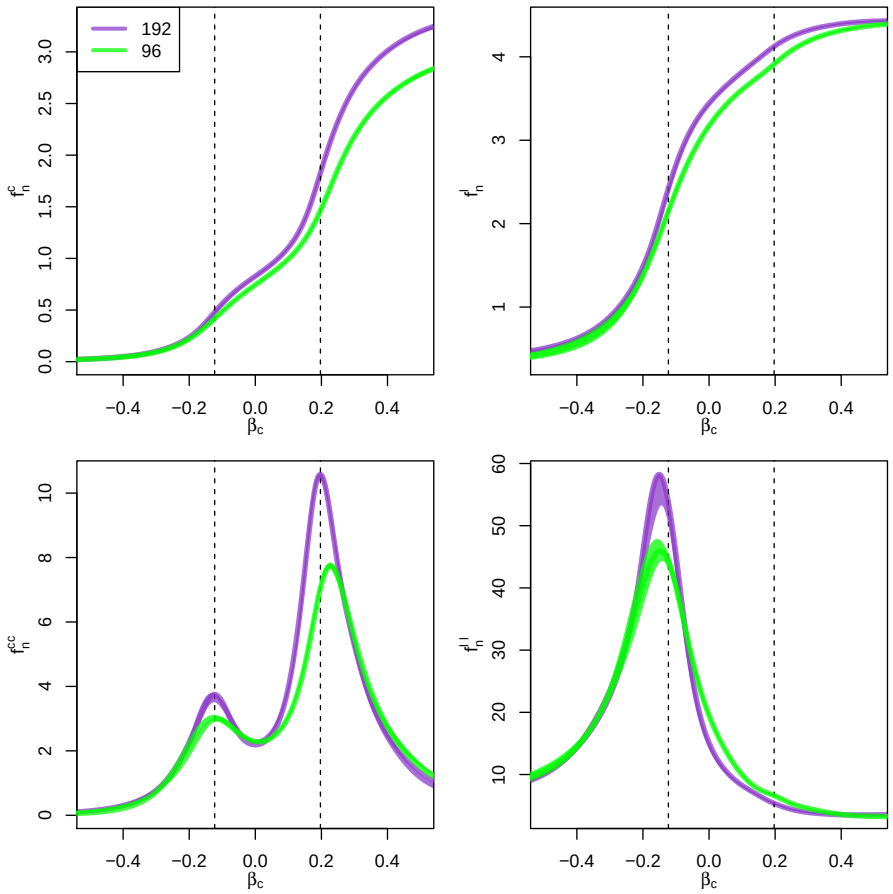

Figure 13. Estimates (f_n^c f_n^l, f_n^{cc} f_n^{ll}) of derivatives of the free energy at $\beta_h = 0.5$, $\beta_l = 0.4$, $\beta_s = 2$ against β_c. The vertical lines mark the positions of the peaks in f_n^{cc}.

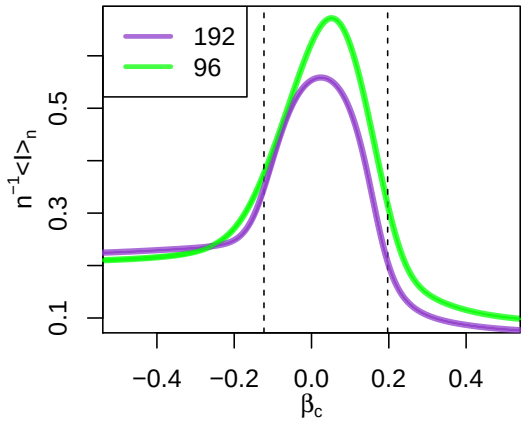

Figure 14. Moment of inertia $n^{-1} \langle I \rangle_n$ at $\beta_h = 0.5$, $\beta_l = 0.4$, $\beta_s = 2$ against β_c.

3.3. Very stiff polymers without pulling

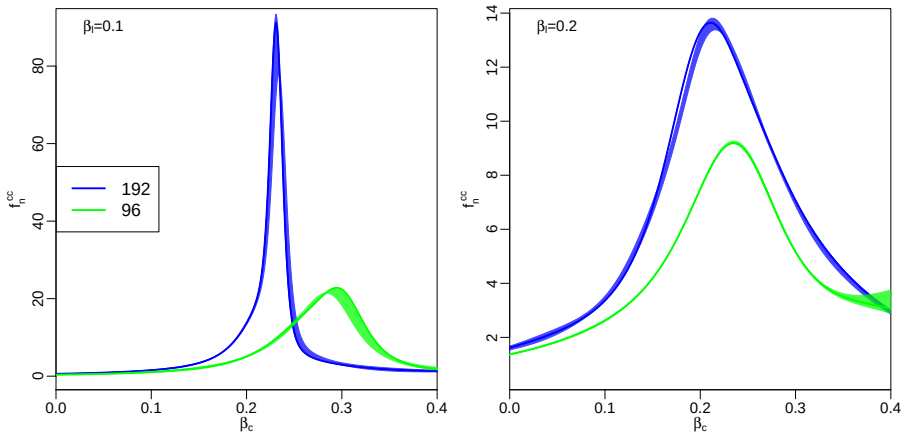

Figure 15. Scaling of $f_n^{cc}\,(\beta_l = const,\, \beta_c,\, \beta_s = 2,\, \beta_h = 0)$ at different torques $\beta_l = 0.1,\, 0.2$.

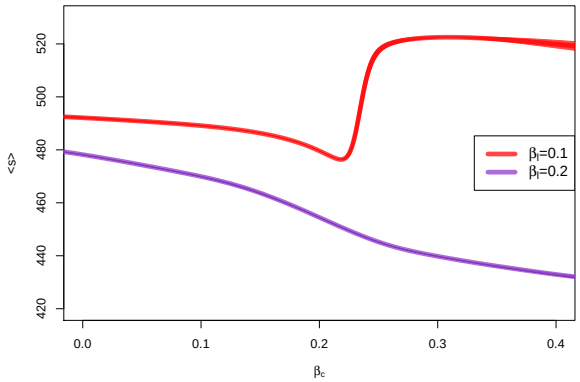

Figure 16. Expectation value of the number of stiff sites against β_c at $n = 192$ for torques $\beta_l = 0.1,\, 0.2$.

Without pulling for a stiff enough lattice polymer, the coil-globule transition becomes the first-order freezing transition into the crystal phase. On the other hand, we expect an applied torque to counteract stiffness as the polymer needs to bend in order to form writhe. This suggests that when the polymer is stiffer than the stiffness at the (coil-globule-crystal) triple point, we may recover a transition into a globule phase by applying torque. Figure 15 provides some support for this idea. It shows the scaling of the contact fluctuations of a semi-flexible polymer ($\beta_s = 2$) with some torque applied. In the model considered in this paper, the critical stiffness lies at about $\beta_s \approx 1.7$. Therefore, we expect to see a crystallization transition as the solvent quality is decreased. At $\beta_l = 0.1$ we find the typical signs of such a transition. The value of the peak in f_n^{cc} more than

doubles when the length is doubled. This suggests a first-order transition. In addition, Figure 16 shows that the expectation value of the number of stiff sites abruptly increases across the transition. At the higher torque value $\beta_l = 0.2$ we do not find these signs of a crystallization transition. Therefore, we assume to observe a transition into the globule phase at $\beta_l = 0.2$. Consequently, we would expect a coil-globule-crystal triple point between $\beta_l = 0.1$ and $\beta_l = 0.2$. However, we have not considered whether this triple point falls together with the conjectured coil-writhed-globule triple point. In general, it appeared to be relatively hard to obtain good results for just semi-flexible polymers.

4. Conclusion

In this paper, we considered an ensemble of geometrically and topologically constrained SAWs on the face-centered cubic lattice. We weighted these SAWs by their writhe and interpreted this as a model of twist storing polymers like DNA. In this framework, the coupling of the writhe is regarded as being related to a torque applied to the DNA. In addition, we also weighted the number of contacts in the SAW by a coupling related to the quality of the solvent. Via simulations, we examined the finite size system for signatures of phase transitions in the coupling space spanned by torque and solvent quality. Our results suggest that weighting the writhe of flexible SAWs induces a second-order phase transition from a coiled phase into a writhed phase. However, this transition is very weak and at the lengths considered here, we were not able to observe it via the moments of the writhe. However, the number of contacts shows weak scaling so that by considering the problem in the torque-solvent quality plane, we were able to conjecture that the transition should lie at $\beta_l \approx 0.3$. In this plane, we conjecture three phases exist: coil or extended, globule and writhed. The first two of these are well known from standard polymer collapse. It will be interesting in the future to investigate more closely the transition into the writhed phase as we were unable to estimate critical exponents. The nature of the point between the three phases would also be of interest.

Then, we considered the case of pulled, semi-flexible polymers. When pulling a SAW the coil (extended) phase immediately becomes a stretched phase with anisotropic size scaling. However, both the globule phase, as has previously been ascertained, and the writhed phase remain. The addition of pulling seems to make the stretched-writhed and stretched-globule transitions more pronounced than their coil-writhed and coil-globule counterparts. In particular, the stretched-globule transition becomes first-order, as is well known. The writhed-globule and stretched-writhed transitions seem to be second-order although our data is once again not sufficient to meaningfully estimate the associated scaling exponents.

Finally, we briefly discussed the case of very stiff polymers, which are known to undergo a first-order freezing transition as the quality of the solvent is reduced. We showed some evidence that by applying torque, this first order transition appears to vanish. Instead, we saw a continuous transition into the perhaps globule phase. Clearly, the stiff regime requires further investigation. We point out that this might be relevant

to experiments on DNA, as the latter is stiff enough to undergo a first-order transition into an ordered (crystal-like) phase when the solvent quality is reduced.

Acknowledgments

One of the authors, ED, gratefully acknowledges the financial support of the University of Melbourne via its Melbourne International Research Scholarships scheme. Financial support from the Australian Research Council via its support for the Centre of Excellence for Mathematics and Statistics of Complex Systems and the Discovery Projects scheme is gratefully acknowledged by one of the authors, ALO.

References

[1] J. Aldinger, I. Klapper, and M. Tabor. Formulae for the calculation and estimation of writhe. *Journal of Knot Theory and Its Ramifications*, 32:37–53, 1995.

[2] U. Bastolla and P. Grassberger. Phase transitions of single semi-stiff polymer chains. *Journal of Statistical Physics*, 89(5-6):1061–1078, 1997.

[3] C. J. Benham. *Mathematics of DNA structure, function and interactions*. The IMA volumes in mathematics and its applications: 150. Dordrecht; New York: Springer, 2009.

[4] C. Bouchiat and M. Mezard. Elastic rod model of a supercoiled DNA molecule. *The European Physical Journal E*, 2(4):377–402, 2000.

[5] H. Brutzer, N. Luzzietti, D. Klaue, and R. Seidel. Energetics at the DNA supercoiling transition. *Biophysical Journal*, 98(7):1267, 2010.

[6] G. Călugâreanu. L'intègrale de gauss et l'analyse des noeuds tridimensionnels. *Revue Roumaine de Mathématiques Pures et Appliquées*, 4:5–20, 1959.

[7] G. Călugâreanu. Sur les classes d'isotopie des noeuds tridimensionnels et leurs invariants. *Czechoslovak Mathematical Journal*, 11:588–625, 1961.

[8] G. Călugâreanu. Sur les enlacements tridimensionnels des courbes fermées. *Communications of the Academia Republicii Populare Romîne*, 11:829–832, 1961.

[9] E. Dagrosa. *Statistical Mechanics of the Lattice Ribbon*. PhD thesis, The University of Melbourne, 2015.

[10] E. Dagrosa and A. L. Owczarek. Generalizing ribbons and the twist of the lattice ribbon. *Journal of Statistical Physics*, 155:392 – 417, 2014.

[11] E. Dagrosa, A. L. Owczarek, and T. Prellberg. Writhe-induced knotting in a lattice polymer. *Journal of Physics A: Mathematical and Theoretical*, 48(6):065002, 2015.

[12] M. Emanuel, G. Lanzani, and H. Schiessel. Multiplectoneme phase of double-stranded DNA under torsion. *Physical Review E*, 88:022706, 2013.

[13] S. Forth, C. Deufel, M. Y. Sheinin, B. Daniels, J. P. Sethna, and M. D. Wang. Abrupt buckling transition observed during the plectoneme formation of individual DNA molecules. *Physical Review Letters*, 100:148301, 2008.

[14] F. B. Fuller. Decomposition of the linking number of a closed ribbon: A problem from molecular biology. *Proceedings of the National Academy of Sciences*, 75(8):3557–3561, 1978.

[15] K. Klenin and J. Langowski. Computation of writhe in modeling of supercoiled DNA. *Biopolymers*, 54(5):307–317, 2000.

[16] W. Kung and R. D. Kamien. Topological constraints at the theta-point: Closed loops at two loops. *Europhysics Letters*, 64(3):323 – 329, 2003.

[17] P.-Y. Lai. First-order phase transition in unfolding a collapsed polymer: A histogram Monte Carlo simulation. *Physical Review E*, 58:6222–6228, 1998.

[18] C. Laing and D. W. Sumners. Computing the writhe on lattices. *Journal of Physics A: Mathematical and General*, 39(14):3535, 2006.

[19] Y. W. Li, T. Vogel, T. Wuest, and D. P. Landau. A new paradigm for petascale Monte Carlo simulation: Replica exchange Wang-Landau sampling. *Journal of Physics: Conference Series*, 510(1):012012, 2014.

[20] J. F. Marko. Supercoiled and braided DNA under tension. *Physical Review E*, 55:1758–1772, 1997.

[21] J. F. Marko and S. Neukirch. Competition between curls and plectonemes near the buckling transition of stretched supercoiled DNA. *Physical Review E*, 85(1):011908, 2012.

[22] J. D. Moroz and R. D. Kamien. Self-avoiding walks with writhe. *Nuclear Physics B*, 506(3):695 – 710, 1997.

[23] S. Sinha and J. Samuel. Biopolymer elasticity: Mechanics and thermal fluctuations. *Physical Review E*, 85:041802, 2012.

[24] S. Sinha and J. Samuel. Statistical mechanics of ribbons under bending and twisting torques *Journal Of Physics: Condensed Matter*, 25(46):465102, 2013.

[25] T. Strick, J.-F. Allemand, V. Croquette, and D. Bensimon. Twisting and stretching single DNA molecules. *Progress in Biophysics and Molecular Biology*, 74(1-2):115 – 140, 2000.

[26] A. Swetnam and C. Brett and M. .P. Allen. Phase diagrams of knotted and unknotted ring polymers *Physical Review E*, 85:031804, 2012

[27] F. Wang and D. P. Landau. Efficient, multiple-range random walk algorithm to calculate the density of states. *Physical Review Letters*, 86:2050–2053, 2001.

[28] J. H. White. Self-linking and the Gauss integral in higher dimensions. *American Journal of Mathematics*, 91(3):pp. 693–728, 1969.

[29] C. Zhou and R. N. Bhatt. Understanding and improving the Wang-Landau algorithm. *Physical Review E*, 72:025701, 2005.